Magnetic and Magnetocaloric Properties of High-Energy Ball-Milled Nanocrystalline $CeMn_2Ge_2$ Compound

MELIKE KAYA, ILKER DINCER, SELCUK AKTURK, and YALCIN ELERMAN

$CeMn_2Ge_2$ nanopowders have been obtained by high-energy ball milling for 5 and 10 hours from bulk compound to investigate the effect of milling time on magnetic and magnetocaloric properties. $CeMn_2Ge_2$ nanopowders have been characterized by X-ray diffraction (XRD), scanning electron microscopy with energy-dispersive X-ray spectroscopy, transmission electron microscopy, and magnetization measurements. The average grain size of the nanoparticles from XRD measurements is about 12.2 and 8 nm for 5-hour and 10-hour ball-milled samples, respectively. The investigations reveal that magnetic entropy change (ΔS_m) can be altered by changing the particle size of the compound. Maximum ΔS_m is -2.45 and -1.30 J kg^{-1} K^{-1} for the 5- and 10-hour ball-milled nanopowders, respectively.

DOI: 10.1007/s11661-016-3661-x

I. INTRODUCTION

INTERMETALLIC RMn_2X_2 (R = rare-earth, X = Si or Ge) compounds have been comprehensively investigated owing to their exciting physical and magnetic properties.[1–7] $CeMn_2Ge_2$ exhibits unusual and attractive properties which crystallize in body-centered tetragonal (space group *I4/mmm*) with Ce, Mn, and Ge atoms located at 2*a*(0,0,0), 4*d*(0, ½, ¼), and 4*e*(0,0,*z*), respectively.[8] The $CeMn_2Ge_2$ compound exposes magnetic moments solely at Mn sites even at the lowest temperatures.[9] $CeMn_2Ge_2$ bulk compound has been studied by multiple methods,[10–15] due to its unexpected magnetic form; nevertheless, there are inadequate data in the literature about nanoformed $CeMn_2Ge_2$ regarding its magnetic or magnetocaloric properties. Decreasing mean crystalline size down to the nanometer scale may suggest both modification of the magnetic properties as far as those of corresponding bulk compositions are concerned and occurrence of new physical properties. High-energy ball milling (HEBM) is a commonly used technique for alloying and mechanical processing of materials.[16–19] In the present study, we focus on the effect of particle size reduction of the intermetallic $CeMn_2Ge_2$ compound obtained by the HEBM technique that has been presented and discussed by their magnetic and magnetocaloric properties.

MELIKE KAYA, Ph.D. Student, and ILKER DINCER and YALCIN ELERMAN, Professors, are with the Department of Engineering Physics, Faculty of Engineering, Ankara University, 06100 Besevler, Ankara, Turkey. Contact e-mail: idincer@eng.ankara.edu.tr SELCUK AKTURK, Professor, is with the Department of Physics, Faculty of Science, Muğla Sıtkı Koçman University, 48000 Kötekli, Turkey.

Manuscript submitted January 15, 2016.
Article published online July 26, 2016

II. EXPERIMENTAL

The bulk $CeMn_2Ge_2$ was produced on a water-cooled arc-melting furnace under argon atmosphere. The purity of the elements was 99.9 pct Ce, 99.98 pct Mn, and 99.98 pct Ge. To compensate the mass loss of Mn, additional 2 pct Mn was added to the stoichiometric amount. To reach homogeneity, the polycrystalline bulk was remelted a few times. The bulk $CeMn_2Ge_2$ compound was grinded then ball-milled using planetary milling system (PULVERISETTE 7) for 5 and 10 hours in the hardened steel vial under ambient atmosphere. Before the milling process, bulk compound was ground using an agate mortar. The rotation speed kept constant at 500 rpm and the weight ratio of sample was around 12:1. To prevent cold welding and overheating (plastic deformation or agglomeration), milling system was stopped every half an hour then continue with the same process.

At room temperature, to characterize the crystal structures, X-ray diffraction data were taken by XRD, RIGAKU D-MAX 2200 diffractometer equipped with Mo Kα radiation for bulk compound and nanopowders. The size and shape of the nanopowders were inspected by SEM (JEOL JSM 7600F at 20 kV) and TEM (JEOL JEM 2100F at 200kV). To find out the elemental composition of the nanopowders, JEOL JSM 7600F equipped with an Oxford EDS was used. For TEM analysis, nanopowders were prepared in ethanol by ultrasonification. The solution was then dropped on amorphous carbon-coated copper grid and was allowed to dry.

The magnetization measurements were made in a vibrating sample magnetometer (VSM, MicroSense EV9) with a sensitivity range of ~10^{-7} emu at room temperature. VSM samples were weighed with a typical digital electronic balance (mass measurement error ±0.1 mg). The temperature dependence of magnetization curves

$M(T)$ was measured in the field-heated (FH) mode at a constant applied field of 800 Oe, in the temperature range from 175 K to 385 K (−98 °C to 112 °C). A Ni standard test sample (4.2 ± 0.1 emu at 1 T) was used to ensure accuracy before each measurement. Magnetic entropy change was calculated by performing magnetic field-dependent magnetization measurements $M(H)$ around Curie temperatures. Data were collected while increasing the applied magnetic field from 0 to 1.8 T at around the transition temperatures with 5 K (5 °C) temperature rising steps.

III. RESULTS AND DISCUSSION

The XRD patterns shown in Figure 1 correspond to the bulk and nanopowders with their Bragg positions, respectively. According to Figure 1, the XRD patterns reveal the single-phase formation for all the investigated samples and well-defined Bragg peaks that could be indexed in a $ThCr_2Si_2$-type tetragonal structure. The refined unit cell parameters (a, c) and unit cell volumes (V) for bulk and nanopowders are listed in Table I. For the size distribution determination, the Scherrer's method[20]

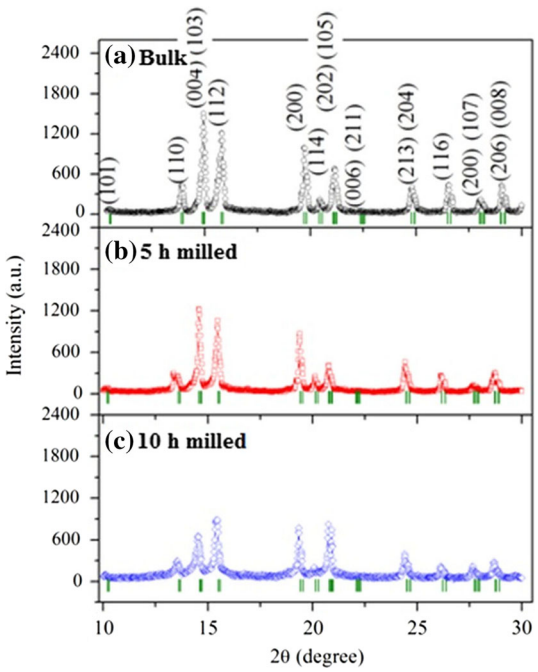

Fig. 1—X-ray powder-diffraction patterns of bulk (crushed in agate mortar) (*a*), 5-h ball-milled (*b*) and 10-h ball-milled (*c*) $CeMn_2Ge_2$ at room temperature.

Table I. The Refined Unit Cell Parameters *a*, *c* and Volume *V* for Bulk (Crushed Sample) and Nanopowders

Sample Type	a (Å)	c (Å)	V (Å^3)
Bulk	4.144(3)	10.931(2)	187.7(3)
5 h Milled	4.147(2)	10.943(2)	188.3(2)
10 h Milled	4.142(3)	10.925(2)	187.5(3)

was applied. Full width at half maximum (FWHM) value of the XRD peaks give information about size distribution in equation of Scherrer's method. Average particle sizes estimated by XRD found 25.0 nm for the starting size of pieces (crushed in agate mortar), 12.2 and 8.0 nm for 5- and 10-hour-milled nanopowders, respectively.

Figures 2(a) and (b) show SEM and TEM micrographs of 5-hour ball-milled $CeMn_2Ge_2$ nanopowders, respectively. The SEM and TEM images show that the diameters of the nanopowders vary between 15 nm to 23 nm. According to EDS results of 5-hour ball-milled $CeMn_2Ge_2$ nanopowders, atomic percentage of sample is 40.02 ± 1.2 wt pct Mn, 37.98 ± 1.3 wt pct Ge, and 22.00 ± 1.4 wt pct Ce.

In addition, SEM and TEM micrograph of 10-hour ball-milled $CeMn_2Ge_2$ nanopowders are shown in Figures 3(a) and (b), respectively. The particle size of this sample varies between 8 nm and 18 nm. It is obtained that atomic percentage of this sample is 40.00 ± 0.8 wt pct Mn, 40.14 ± 0.9 wt pct Ge, and 19.86 ± 1.0 wt pct Ce(wt).

SEM, TEM, and EDS analysis results reveal that 5-hour and 10-hour ball-milled nanoparticles are both different in size and practically have spherical morphology.

The average sizes of the nanopowders were also calculated using the FWHM of the XRD peaks in Scherrer's formula and results are compatible to that obtained by TEM and SEM. In addition, the EDS results confirmed that the molar ratio of Ce:Mn:Ge was 1:2:2 as expected for both 5- and 10-hour ball-milled samples.

In order to investigate the magnetic behavior of the samples, temperature-dependent magnetization measurements, $M(T)$, were carried out for 5- and 10-hour ball-milled samples under 800 Oe, consistent with that used in the bulk one to compare saturation magnetization values.[8] The $M(T)$ curves, measured from 175 K to 385 K (−98 °C to 112 °C) in a magnetic field of 800 Oe for field-heated FH mode, are displayed in Figure 4.

Results of magnetization measurements as a function of temperature show almost identical behavior for different milling times. According to Figure 4, milled nanopowders are ferromagnetic below T_c = 318 K (45 °C). Decrease in T_c compared to bulk is associated with the milling process. These results are due to the strength of the Ce-Ce magnetic interactions and arrangements of the Mn magnetic moments. The magnetic properties of bulk $CeMn_2Ge_2$ have been previously studied by magnetic measurements (below T_c), using Mössbauer and neutron diffraction techniques.[9,11,12,14,21] Additionally, below the Curie temperature, there is a small maximum in the FH curves for both nanopowders at about 278 K (5 °C). This transition temperature, related to the transition temperature ($T_{C/C}$), which is also observed by magnetic measurements in the bulk sample at 284 K (11 °C), arises from canted ferromagnetic to conical ferromagnetic structure of the Mn sublattice.[14]

The phase transition temperatures, T_c and $T_{C/C}$, are lower than that of bulk $CeMn_2Ge_2$ compound. According to Figure 4, $T_{C/C}$ peak can be more easily

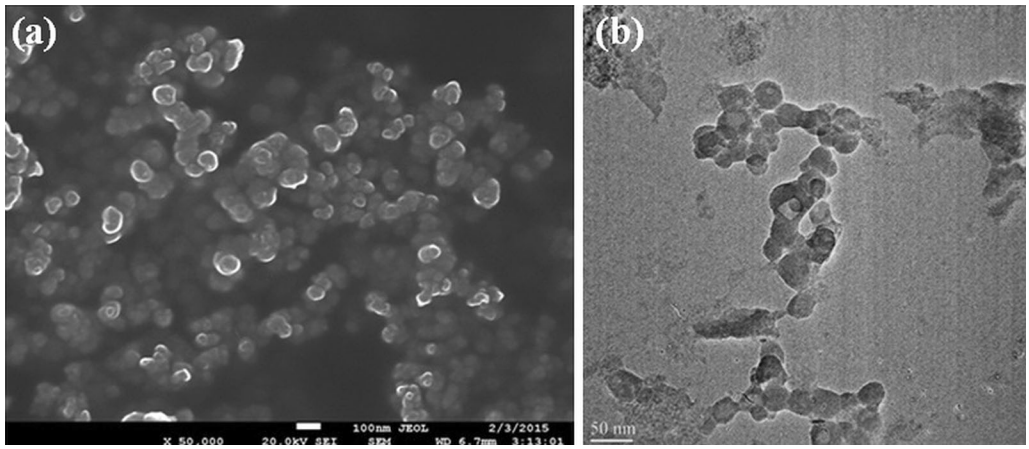

Fig. 2—SEM micrograph (*a*) and TEM micrograph (*b*) of 5-h ball-milled $CeMn_2Ge_2$ nanopowders.

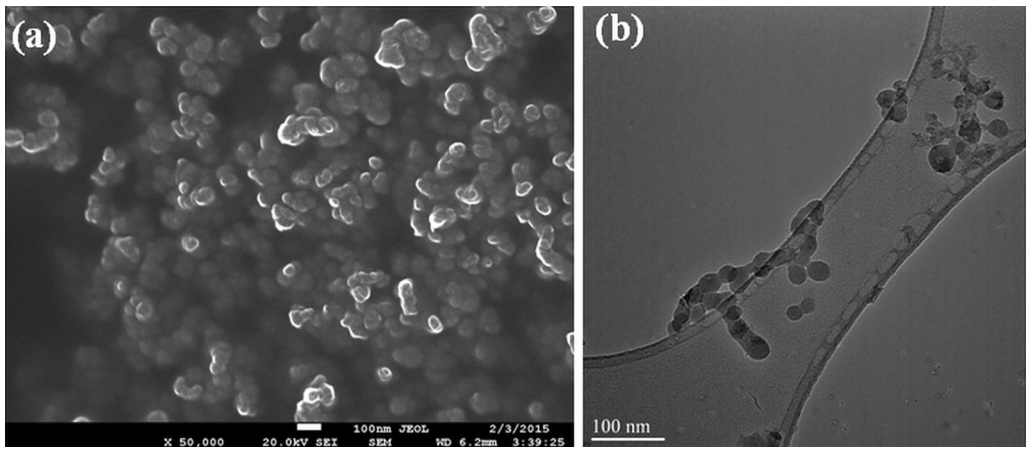

Fig. 3—SEM micrograph (*a*) and TEM micrograph (*b*) of 10-h ball-milled $CeMn_2Ge_2$ nanopowders.

distinguished in the nanopowder than bulk alloy.[9] It should be mentioned that changing the particle size may change transition temperatures in other rare-earth and magnetic compounds. For example, $LaMn_2Si_2$,[18] $CoMnGe_{0.95}Ga_{0.05}$,[19] and $NdMn_2Ge_2$[22] systems shows similar tendency of decreasing T_c from bulk to ball-milled compounds. It is also worth noting that due to the reduction in the grain size and atomic ordering at the surface, the obtained saturation magnetization value for the 5-hour-milled sample is almost half of that for the 10-hour-milled one.

Magnetic field-dependent magnetization, $M(H)$, curves for high-energy ball-milled powder samples are measured around T_c for the increasing and decreasing magnetic field (Figures 5(a) and (b)). As shown in Figures 5(a) and (b), the magnetization increases but do not rapidly saturates at low magnetic field. The magnetic entropy change around the magnetic transition temperature (Figure 6) is calculated from $M(H)$ curves using the integrated Maxwell relation:

$$\Delta S_m = \int_{H_1}^{H_2} \left(\frac{\partial M}{\partial T}\right)_H dH, \qquad [1]$$

From which the magnetocaloric effect can be estimated by numerical integration using the data in Figures 5(a) and (b). The sign of ΔS_m is negative for all temperatures, indicating that conventional magnetocaloric effect is present, i.e., the sample heats when a magnetic field is applied adiabatically as in the $NdMn_2Ge_2$[22] and $SmMn_2Si_2$[23] alloys. The uncertainty is estimated 5.0 pct in the determination of each data in magnetic entropy change (Figure 6) for the nanopowders.

The maximum values of $|\Delta S_m|$ for ball-milled samples are 2.45 and 1.30 J kg^{-1} K^{-1} for the 5- and 10-hour-milled nanopowders under the magnetic field change of 1.8 T, respectively. 5-hour-milled nanopowders exhibit larger $|\Delta S_m|$ value in contrast to the bulk sample[24] with lower temperature range (Figure 6, inset). In fact, physical and magnetic properties of nanopowders arise from unique interaction between particles. Consequently, magnetocaloric properties can be controlled by geometry and volume fraction of samples.

Magnetic refrigerants are required to display another important characteristic parameter, namely the relative cooling power (RCP). It is necessary to take into account the RCP value which is determined by the

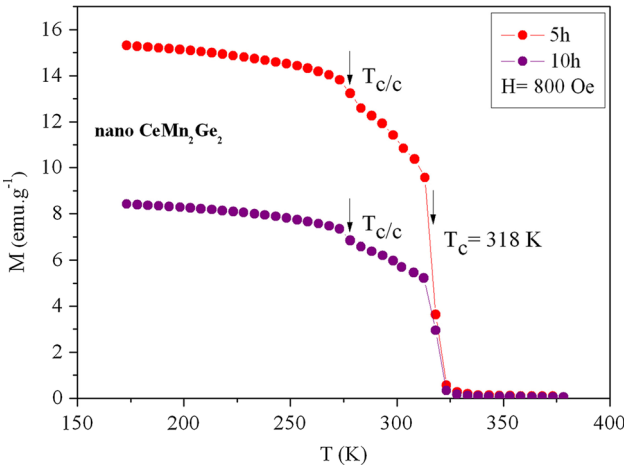

Fig. 4—The $M(T)$ curves for nanostructured 5- and 10-h-milled sample in magnetic field of 800 Oe.

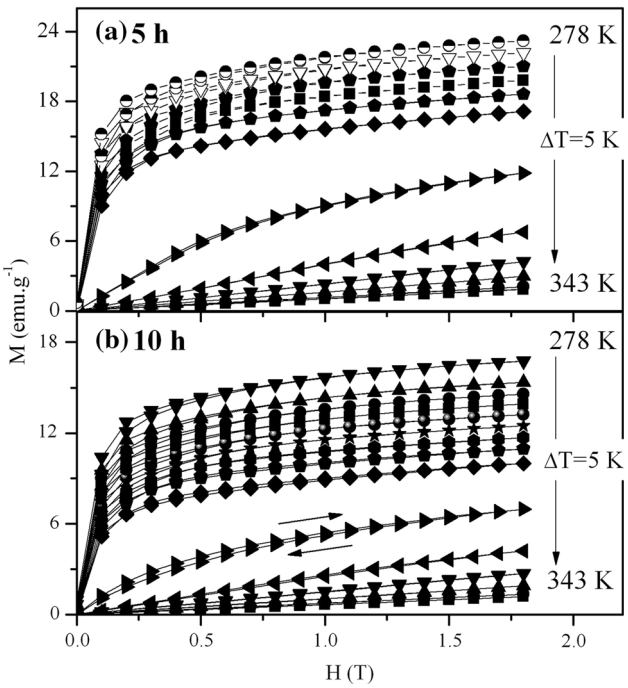

Fig. 5—The $M(H)$ curves for 5- (*a*) and 10-h (*b*)-milled samples measured from 0 to 1.8 T.

peak value of the entropy change ΔS_m and the full width at half maximum (FWHM) of ΔT and written as

$$\mathrm{RCP} = -\Delta S_m \cdot \Delta T_{\mathrm{FWHM}}. \qquad [2]$$

By using Eq. [2], RCP values are found to be 22.1 and 13.0 J kg^{-1} for an applied field of 1.8 T for 5- and 10-hour ball-milled samples, respectively. Considering the fact that the observed magnetic entropy change values with their magnitudes are quite important when compared to the some other intermetallic bulk compounds such as $PrMn_2Ge_{0.8}Si_{1.2}$,[25] $Nd(Mn_{0.8}Fe_{0.2})_2Ge_2$,[26] and $La_{0.65}Ce_{0.35}Mn_2Si_2$,[27] the obtained RCP values around Curie temperature for investigated

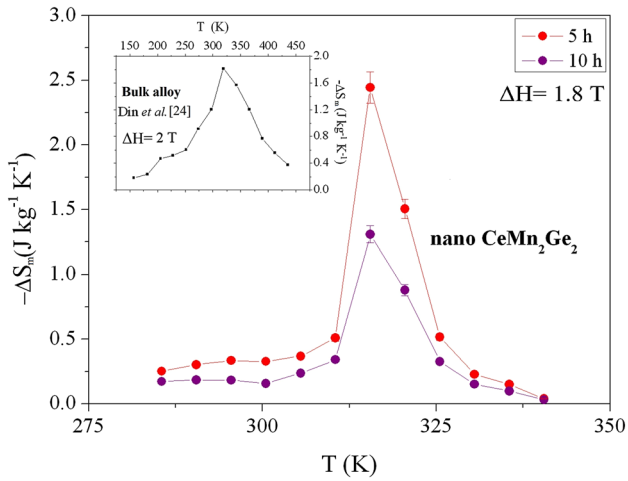

Fig. 6—The temperature dependence of the magnetic entropy changes of the 5- and 10-h-milled $CeMn_2Ge_2$ nanopowders for 1.8 T. Inset Din *et al.* found ΔS_m value of bulk $CeMn_2Ge_2$ alloy at magnetic field change of 2 T.[24]

ball-milled nanopowders are lower than those of bulk $PrMn_2Ge_{0.8}Si_{1.2}$,[25] $Nd(Mn_{0.8}Fe_{0.2})_2Ge_2$,[26] and $La_{0.65}Ce_{0.35}Mn_2Si_2$[27] but very close to the reported 5-hour ball-milled $NdMn_2Ge_2$[22] alloy. Short-time heat treatment or substitution of some other forth element to change magnetic interaction between Mn-Mn atoms can modify magnetic cooling properties.

IV. CONCLUSIONS

In conclusion, we have studied the effect of ball milling time on the magnetic and magnetocaloric properties of the $CeMn_2Ge_2$ sample. Saturation magnetization values, magnetic entropy changes, and RCP values decrease considerably with increasing milling time. According to TEM investigations, the particle size of the nanoparticles changes from 15 to 23 and 8 to 18 nm for 5- and 10-hour-milled nanoparticles, respectively. A peak is observed for both samples in $M(T)$ curves at about 278 K (5 °C) which is related to magnetic structure for Mn sublattice, consistent with previous experiments.[21] Furthermore, the observed Curie temperature [T_c = 318 K (45 °C)] is independent of the milling time. The magnetic entropy change values of nanopowders are −2.45 J kg^{-1} K^{-1} and −1.30 J kg^{-1} K^{-1} around T_C at 1.8 T magnetic field change for 5- and 10-hour samples, respectively. Also, the relative cooling powers of investigated ball-milled sample are 22.1 and 13.0 J kg^{-1} at 1.8 T for 5- and 10-hour samples, respectively.

REFERENCES

1. J.H.V.J. Brabers, K. Bakker, H. Nakotte, F.R. de Boer, S.K.J. Lenczowski, and K.H.J. Buschow: *J. Alloys Compd.*, 1993, vol. 199, pp. L1–L3.
2. R.B. van Dover, E.M. Gyorgy, R.J. Cava, J.J. Krajewski, R.J. Felder, and W.F. Peck: *Phys. Rev. B*, 1993, vol. 47, pp. 6134–37.

3. E. Duman, M. Acet, I. Dincer, A. Elmali, and Y. Elerman: *J. Magn. Magn. Mater.*, 2007, vol. 309, pp. 40–53.
4. I. Dincer and Y. Elerman: *J. Magn. Magn. Mater.*, 2013, vol. 326, pp. 50–57.
5. K.S.V.L. Narasimhan, V.U.S. Rao, R.L. Bergner, and W.E. Wallace: *J. Appl. Phys.*, 1975, vol. 46, p. 4957.
6. H. Kobayashi, H. Onodera, and H. Yamamoto: *J. Magn. Magn. Mater.*, 1989, vol. 79, p. 76.
7. S.J. Campbell, J.M. Cadogan, X.L. Zhao, M. Hofmann, and H.S. Li: *J. Phys. Condens. Matter*, 1999, vol. 11, pp. 7835–50.
8. Z. Ban and M. Sikirica: *Acta Cryst.*, 1965, vol. 18, p. 594.
9. S. Kervan, M. Acet, and Y. Elerman: *Solid State Commun.*, 2001, vol. 119, pp. 95–99.
10. A. Szytuła and S. Siek: *J. Magn. Magn. Mater.*, 2007, vol. 27, pp. 49–54.
11. R. Welter, G. Venturini, E. Ressouche, and B. Malaman: *J. Alloys Compd.*, 1995, vol. 218, pp. 204–15.
12. I. Nowik, Y. Levi, I. Felner, and E.R. Bauminger: *J. Magn. Magn. Mater.*, 1995, vol. 147, pp. 373–84.
13. A. Elmali, I. Dincer, Y. Elerman, H. Ehrenberg, and H. Fuess: *J. Phys.: Condens. Matter*, 2003, vol. 15, pp. 653–61.
14. O. Cakir, I. Dincer, A. Elmali, E. Duman, and Y. Elerman: *J. Magn. Magn. Mater.*, 2005, vol. 295, pp. 235–40.
15. M. Kabak, A. Elmali, I. Dincer, and Y. Elerman: *Solid State Commun.*, 2004, vol. 132, pp. 31–35.
16. B. Chevalier, J.-L. Bobet, J.S. Marcos, J.R. Fernandez, and J.C.G. Sal: *Appl. Phys. A*, 2005, vol. 80, pp. 601–06.
17. T. Zhang, Y. Chen, and Y. Tang: *J. Phys. D Appl. Phys.*, 2007, vol. 40, pp. 5778–84.
18. A. Elmali, S. Tekerek, I. Dincer, Y. Elerman, R. Theissmann, H. Ehrenberg, and H. Fuess: *J. Magn. Magn. Mater.*, 2008, vol. 320, pp. 364–67.
19. E. Yüzüak, G. Durak, I. Dincer, and Y. Elerman: *J. Alloys Comp.*, 2012, vol. 541, pp. 256–62.
20. A. Patterson: *Phys. Rev.*, 1939, vol. 56, pp. 978–82.
21. J.A. Fernandez-Baca, P. Hill, B.C. Chakoumakos, and N. Ali: *J. Appl. Phys.*, 1996, vol. 79, pp. 5398–400.
22. M. Kaya, M. Rezaeivala, E. Yüzüak, S. Akturk, I. Dincer, and Y. Elerman: *Phys. Status Solidi B*, 2015, vol. 252, pp. 192–97.
23. P. Kumar, K.G. Suresh, A.K. Nigam, and S.K. Malik: *J. Appl. Phys.*, 2008, vol. 103, p. 013909.
24. M.F. Md Din, J.L. Wang, Z.X. Cheng, S.X. Dou, S.J. Kennedy, M. Avdeev, and S.J. Campbell: *Sci. Rep.*, 2015, vol. 5, pp. 1–15.
25. J.L. Wang, S.J. Campbell, R. Zeng, C.K. Poh, S.X. Dou, and S.J. Kennedy: *J. Appl. Phys.*, 2009, vol. 105, p. 07A909.
26. Y.Q. Chen, J. Luo, J.K. Liang, J.B. Li, and G.H. Rao: *J. Alloys Compd.*, 2010, vol. 489, pp. 13–19.
27. B. Emre, I. Dincer, and Y. Elerman: *J. Magn. Magn. Mater.*, 2010, vol. 322, pp. 448–53.